Acta Cryst. (1999). B**55**, 313–320

The crystal structure of $Ca_7Zr_7Ta_6O_{36}$ refined using synchrotron-radiation data

Siegbert Schmid,[a]* John G. Thompson,[a] Ray L. Withers,[a] Christopher D. Ling,[a] Nobuo Ishizawa[b] and Shunji Kishimoto[c]

[a]*Research School of Chemistry, Australian National University, GPO Box 414, Canberra, ACT 2601, Australia,* [b]*Materials and Structures Laboratory, Tokyo Institute of Technology, Nagatsuta, Midori-ku, Yokohama 226, Japan, and* [c]*National Laboratory for High Energy Physics, Oho, Tsukuba 305, Japan. E-mail: schmid@rsc.anu.edu.au*

(*Received 2 July 1998; accepted 2 November 1998*)

Abstract

Single-crystal X-ray diffraction data [synchrotron radiation; λ = 1.2682 (4) Å] are used to solve and refine the crystal structure of heptacalcium hexatantalum heptazirconium hexatriacontaoxide, $Ca_7Zr_7Ta_6O_{36}$. The structure adopts space group *Fddd* with cell dimensions a = 36.394 (1), b = 7.3674 (5), c = 31.006 (2) Å. The structure was solved by direct methods. Refinement using 1299 unique reflections leads to final values of R = 0.031 and wR = 0.034. The refined metal-atom ordering scheme is far from fully ordered and reminiscent of the A/B metal-atom ordering characteristic of the pyrochlore structure type. Bond-valence sums are calculated to confirm the plausibility of the crystal chemistry of $Ca_7Zr_7Ta_6O_{36}$.

1. Introduction

In a recent study of the $LiTaO_3$–$CaZrO_3$ pseudo-binary phase diagram with the aim of investigating the structural origin of a reported two-phase region, a previously unreported long-period superstructure phase (Schmid *et al.*, 1996) was observed. Strong subcell reflections in electron and X-ray powder diffraction patterns of this phase indicated a close relationship to the fluorite structure type. A combination of electron diffraction and Guinier–Hägg X-ray powder diffraction led to the assignment of unit-cell dimensions a = 36.372 (3), b = 7.3590 (5), c = 31.018 (8) Å and space group *Fddd*. The cell corresponds to a 10 × 2 × 6 superstructure of an underlying *I*-centred fluorite-type parent structure (Fig. 1).

The composition determined by energy-dispersive spectroscopy in a scanning electron microscope was 0.304 (4)$TaO_{2.5}$·0.347 (4)ZrO_2·0.349 (4)CaO (Schmid *et al.*, 1996). A very small amount of a ZrO_2-rich phase was also detected in a back-scattered electron image. It was shown that for a fully ordered cation array derived from a fluorite-type structure the composition ought to be $Ca_7Zr_7Ta_6O_{36}$, *i.e.* 0.30$TaO_{2.5}$·0.35ZrO_2·0.35CaO. This hypothesis appeared to be valid, as synthesis at that ideal composition resulted in the superstructure phase without any apparent traces of an impurity phase.

From a modulated-structure point of view the strongest satellite reflections present in electron diffraction patterns are of the form $\mathbf{G}_F \pm [404]^*$ and $\mathbf{G}_F \pm [913]^*$, where $\mathbf{G}_F$ represents a strong fluorite subcell reflection. Both types of modulation wave vectors fall close to $\frac{1}{2}[111]^*_F$ suggesting a relationship to cubic stabilized zirconias (CSZs) over certain composition ranges (Michel *et al.*, 1974; van Dijk *et al.*, 1986; Miida *et al.*, 1994, 1997) and to the φ^1 phase of Allpress *et al.* (1975), which also show additional scattering in similar regions of reciprocal space. The nominal 10% oxygen-vacancy concentration observed for $Ca_7Zr_7Ta_6O_{36}$ is at the same level as the φ^1 phase and represents one possible vacancy concentration for Ca-, Mg- and Y-stabilized cubic zirconias. Refinement of the crystal structure of $Ca_7Zr_7Ta_6O_{36}$ can thus be expected to give insight into metal and oxygen-vacancy ordering in CSZs.

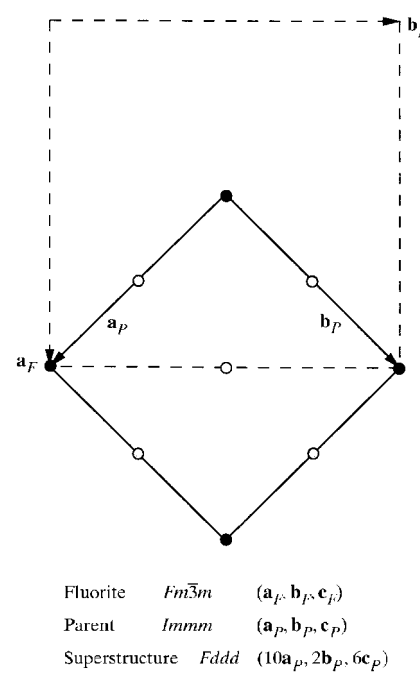

Fig. 1. The relationship of the fluorite unit cell to the parent unit cell and the real cell of $Ca_7Zr_7Ta_6O_{36}$ (black: metal atom at height 0; white: metal atom at height $\frac{1}{2}$; grey: O atom).

Table 1. *Experimental details*

Crystal data	
Chemical formula	$Ca_7Zr_7Ta_6O_{36}$
Chemical formula weight	2580.78
Cell setting	Orthorhombic
Space group	*Fddd*
a (Å)	36.394 (1)
b (Å)	7.3674 (5)
c (Å)	31.006 (2)
V (Å^3)	8313.2 (12)
Z	12
D_x (Mg m^{-3})	6.186
Radiation type	Synchrotron X-ray
Wavelength (Å)	1.2682 (4)
No. of reflections for cell parameters	24
θ range (°)	16.5–24
μ (mm^{-1})	42.71
Temperature (K)	293
Crystal colour	White
Data collection	
Diffractometer	Tsukuba BL14A
Data collection method	$\theta/2\theta$ scans
Absorption correction	None
No. of measured reflections	12 337
No. of independent reflections	1928
No. of observed reflections	1299
Criterion for observed reflections	$I > 2\sigma(I)$
R_{int}	0.039
θ_{max} (°)	50.05
Range of h, k, l	$-44 \rightarrow h \rightarrow 43$ $-8 \rightarrow k \rightarrow 8$ $-34 \rightarrow l \rightarrow 37$
No. of standard reflections	9
Intensity decay (%)	0
Refinement	
Refinement on	F
R	0.031
wR	0.034
S	1.508
No. of reflections used in refinement	1299
No. of parameters used	195
Weighting scheme	$w = 1/[\sigma^2(F) + 0.0001F^2]$
$(\Delta/\sigma)_{max}$	0.021
$\Delta\rho_{max}$ (e Å^{-3})	1.405
$\Delta\rho_{min}$ (e Å^{-3})	−2.081
Extinction method	None

We have been able to grow single crystals of $Ca_7Zr_7Ta_6O_{36}$ large enough to collect synchrotron X-ray diffraction data and the purpose of this paper is to report the results of the structure solution and refinement.

2. Experimental

2.1. *Synthesis*

Single crystals of $Ca_7Zr_7Ta_6O_{36}$ were grown by heating mechanically mixed component oxides at the above stoichiometry at 1623 K in air for 24 h, regrinding and subsequent prolonged tempering at 1623 K in air.

2.2. *Single-crystal intensity-data collection*

Preliminary tests of crystal quality, *e.g.* measurement of reflection profiles, were performed on a Rigaku AFC-6*R* four-circle diffractometer with a rotating Cu anode. The crystals were mounted on tapered glass fibres with the diameter of the fibre ends being approximately the same size as the crystals. The crystal chosen for intensity measurements approximated a square prism of dimensions $15 \times 10 \times 6$ μm (9×10^2 μm^3).

The intensity measurements were carried out using the four-circle diffractometer at BL14A of the Photon Factory, Tsukuba, Japan (Satow & Iitaka, 1989). Synchrotron radiation from a vertical wiggler was monochromated by an Si(111) double-crystal monochromator and focused using a curved mirror. The polarization ratio, *i.e.* the fraction of the total incident beam intensity with its electric vector vertical, is 0.95. In order to determine the location of the Ta L_{III} absorption edge precisely prior to intensity-data collection, a near-edge absorption spectrum of 10 μm-thick Ta foil was recorded. The location of the Ta absorption edge was used to calibrate the monochromator angles with respect to the absolute incident energy. The precision of this value is limited by the width of the absorption edge, which spans several eV in our experimental data. The edge was defined as the monochromator position that corresponded to the point where absorption had risen half way to its far-edge value. All other settings of the incident X-ray energy were defined relative to this value. Decay of the incident beam and spontaneous fluctuations were monitored with an ion chamber to enable normalization of the raw counts. There was no significant change in intensity once the data had been corrected for the variation of the incident beam resulting from decay of the synchrotron ring current.

Intensity data were recorded using an avalanche photodiode detector (Kishimoto *et al.*, 1998). BL14A software was used for the data collection and cell refinement. The relevant parameters for the data collection are given in Table 1. To improve counting statistics for the weaker reflections scans were repeated if $\sigma(F)/F$ was larger than 0.01, where $\sigma(F)$ was calculated from counting statistics only. The maximum number of scans was 3. The data were corrected for Lorentz and polarization effects. No absorption correction was necessary because of the small crystal size. Symmetry-equivalent reflections were averaged in Laue group *mmm* (see Table 1).

3. Structure solution and refinement

The space group of $Ca_7Zr_7Ta_6O_{36}$ was determined from electron diffraction patterns as *Fddd* (Schmid *et al.*,

Table 2. *Metal-ordering models for $Ca_7Zr_7Ta_6O_{36}$ and R values*

	Site	Model 1	Model 2	Model 3	Model 3 electron count
*M*1	16*e*	Ta	Ta	0.64 (2)Ta/0.36 (2)Zr	61
*M*2	16*e*	Ta	Ta	0.85 (2)Ta/0.15 (2)Zr	68
*M*3	32*h*	Ta	Ta	0.81 (2)Ta/0.19 (2)Zr	67
*M*4	32*h*	Zr	0.75Zr/0.25Ta	0.45 (2)Ta/0.55 (2)Zr	55
*M*5	16*e*	Zr	Zr	0.22 (2)Ta/0.78 (2)Zr	47
*M*6	32*h*	Zr	Zr	0.14 (2)Ta/0.86 (2)Zr	45
*M*7	32*h*	Ca	Ca	0.18 (2)Zr/0.82 (2)Ca	24
*M*8	32*h*	Ca	0.625Ca/0.375Zr	0.09 (2)Zr/0.91 (2)Ca	22
*M*9	16*e*	Ca	Ca	0.21 (2)Zr/0.79 (2)Ca	24
*M*10	16*e*	Ca	Ca	0.00 (2)Zr/1.00 (2)Ca	20
R		0.122	0.100	0.061	
wR		0.153	0.126	0.070	

Table 3. *Reflection classes*

Reflections	Observed	$I > 2\sigma(I)$	Unique	$R_{int}(F^2)$	$\sum F_{obs}$ (%)
All	12337	6477	1928	0.039	
Parent	336	209	66	0.034	25.1
First order [404]	1599	1119	256	0.042	29.4
First order [913]	872	796	128	0.029	17.7
Rest/even	3868	1387	658	0.064	8.7
Rest/odd	5662	2966	820	0.076	19.1

Table 4. *Fractional atomic coordinates and equivalent isotropic displacement parameters ($Å^2$)*

$$U_{eq} = (1/3)\Sigma_i\Sigma_j U^{ij} a^i a^j \mathbf{a}_i.\mathbf{a}_j.$$

	Site	*x*	*y*	*z*	Occupancy	U_{eq}
*M*1	16*e*	0.01975 (2)	3/8	7/8	0.62 (2)Ta/0.38 (2)Zr	0.0045 (4)
*M*2	16*e*	0.02395 (2)	3/8	3/8	0.85 (2)Ta/0.15 (2)Zr	0.0039 (4)
*M*3	32*h*	0.074378 (18)	0.12299 (8)	0.458627 (14)	0.81 (2)Ta/0.19 (2)Zr	0.0039 (3)
*M*4	32*h*	0.12253 (2)	0.36635 (8)	0.202284 (18)	0.45 (2)Ta/0.55 (2)Zr	0.0065 (3)
*M*5	16*e*	0.06757 (3)	1/8	1/8	0.22 (2)Ta/0.78 (2)Zr	0.0113 (5)
*M*6	32*h*	0.03224 (2)	0.37420 (16)	0.03484 (2)	0.14 (2)Ta/0.86 (2)Zr	0.0069 (4)
*M*7	32*h*	0.07788 (5)	0.1453 (3)	0.29208 (6)	0.18 (2)Zr/0.82 (2)Ca	0.0228 (10)
*M*8	32*h*	0.02322 (5)	0.8705 (4)	0.03899 (5)	0.09 (2)Zr/0.91 (2)Ca	0.0086 (8)
*M*9	16*e*	0.11849 (7)	3/8	7/8	0.21 (2)Zr/0.79 (2)Ca	0.0230 (12)
*M*10	16*e*	0.07446 (7)	5/8	1/8	0.00 (2)Zr/1.00 (2)Ca	0.0047 (11)
O1	16*g*	1/8	5/8	0.0725 (2)		0.006 (4)
O2	32*h*	0.01909 (16)	0.5821 (8)	0.0803 (2)		0.008 (3)
O3	32*h*	0.02361 (15)	0.1223 (10)	−0.1005 (2)		0.013 (3)
O4	32*h*	0.03071 (17)	0.1449 (11)	−0.0002 (2)		0.011 (3)
O5	32*h*	0.08503 (17)	0.4303 (8)	0.0020 (2)		0.009 (3)
O6	32*h*	0.0761 (2)	0.9129 (9)	0.0834 (2)		0.017 (4)
O7	32*h*	0.08621 (18)	0.8215 (8)	−0.0001 (2)		0.011 (3)
O8	32*h*	0.02478 (14)	0.6069 (11)	−0.0139 (2)		0.009 (3)
O9	32*h*	0.06362 (18)	0.4293 (8)	−0.0840 (2)		0.012 (3)
O10	16*g*	1/8	1/8	0.0155 (3)		0.018 (5)
O11	32*h*	0.01802 (18)	0.1812 (9)	0.0855 (2)		0.014 (4)
O12	16*g*	1/8	5/8	−0.0665 (3)		0.016 (4)
O13	32*h*	0.0794 (2)	0.3315 (9)	0.0800 (2)		0.019 (4)
O14	32*h*	0.0627 (2)	0.8242 (9)	−0.0820 (2)		0.018 (4)
O15	16*g*	1/8	1/8	−0.0847 (3)		0.030 (6)
O16	16*g*	1/8	1/8	0.0989 (5)		0.070 (10)

1996) and the extinction conditions consistent with this space group are confirmed by the intensity data set collected here [only 4 of 831 *d*-glide forbidden reflections have intensities slightly above $3\sigma(I)$]. As will be discussed below, it seems astonishing that $Ca_7Zr_7Ta_6O_{36}$ crystallizes in *Fddd*, as complete metal ordering is not possible in this space group. In fact the symmetry needs to be lowered to *F222* before a metal-ordering pattern is possible where all sites are fully occupied by one type of metal only. The absence of any significant diffuse intensity in electron diffraction patterns suggests a random disorder of the metal array.

The structure solution and refinement were carried out in space group *Fddd* (No. 70; origin choice 2; *International Tables for Crystallography*, Vol. A, 1995) using *Xtal*3.4 (Hall *et al.*, 1995) and *SHELX*97 (Sheldrick, 1997). Scattering factors for neutral atoms were taken from *International Tables for X-ray Crystallography* (Vol. IV, 1974). The dispersion corrections $\Delta f'$ and $\Delta f''$ for Ca, Zr, Ta and O were calculated using the computer program *FPRIME* of Cromer & Liberman (1981). Corrections to the relativistic part of the anomalous-scattering factors were made following Kissel & Pratt (1990). Refinement using full-matrix least squares was on *F*. An additional uncorrelated error of 0.01 was included with the counting statistic estimate in the evaluation of weights.

The structure was solved using direct methods in *Xtal*3.4 (Hall *et al.*, 1995) and *SHELX*97 (Sheldrick, 1997). Owing to the underlying fluorite-related substructure, it proved impossible to distinguish *a priori* between a variety of solutions that gave reasonable and somewhat similar metal-atom positions. Instead it was necessary to pursue any one metal-position arrangement to a point where a decision could reasonably be made, employing comparative refinement strategies. While most of the tested metal-position arrangements refined reasonably well, it was often not possible to extract the required number of O-atom positions from difference Fourier maps and *R* values did not drop below ~0.1. Eventually one metal-position arrangement was established that led to the final result and that process is described in more detail below.

Starting off with the highest peak from direct methods, metal-atom positions were added one by one and confirmed using successive Fourier maps. Metal atoms were assigned to particular sites according to the height of corresponding peaks in the Fourier maps. Comparative refinements were employed to establish an unambiguous metal-atom ordering scheme with all metal sites fully occupied by one or other type of metal ion ($R \simeq 0.19$). This metal-ion arrangement yielded O-atom positions quite readily from subsequent difference Fourier maps. Both metal and O atoms were given isotropic atomic displacement parameters (model 1, Table 2). Model 1, however, does not correspond to the correct stoichiometry. Therefore, two of the metal positions were chosen as sites with mixed occupancies (Ta on the *M*4 site, Zr on the *M*8 site), according to the stoichiometry, because they had non-positive definite or

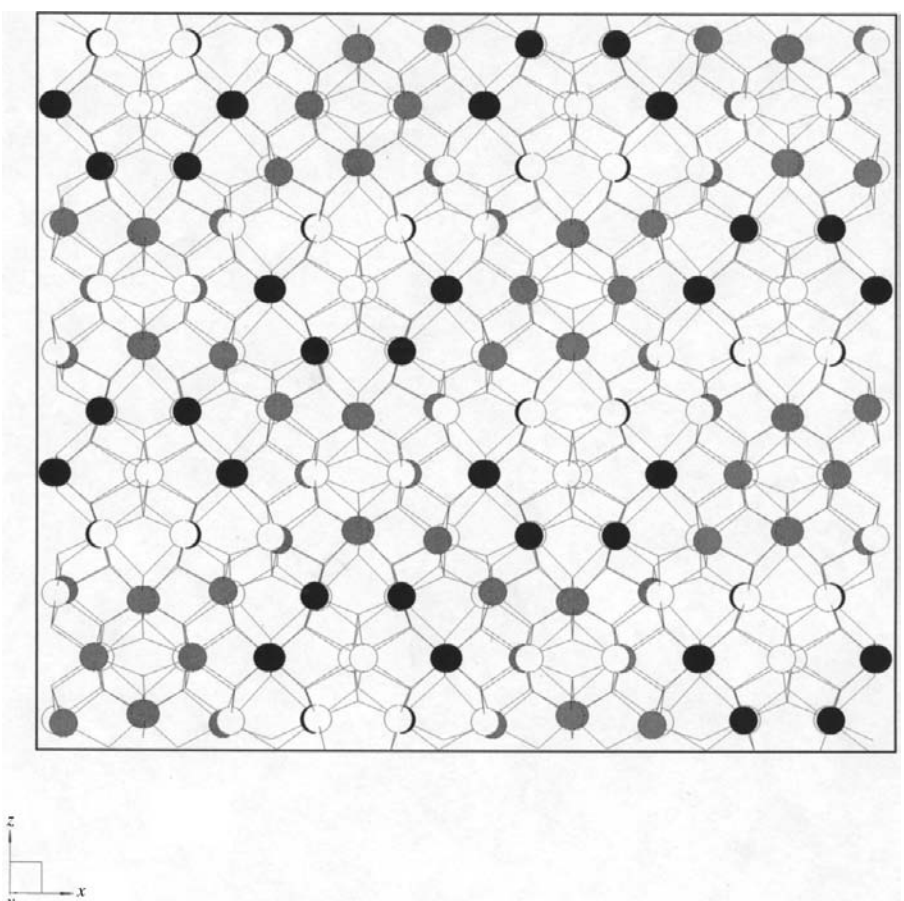

Fig. 2. The final structure of $Ca_7Zr_7Ta_6O_{36}$ projected down **b** (*M*1–*M*3: black; *M*4–*M*6: grey; *M*7–*M*10: white, corresponding roughly to the electron count). Lines correspond to *M*—O bonds < 3.2 Å, O atoms are at the bond intersections.

Table 5. *Bond-valence sums for* $Ca_7Zr_7Ta_6O_{36}$

	All Ta	All Zr	All Ca
*M*1	4.432	4.640	5.032
*M*2	5.070	5.308	5.756
*M*3	4.933	5.164	5.601
*M*4	4.445	4.654	5.047
*M*5	4.345	4.549	4.933
*M*6	3.574	3.742	4.058
*M*7	2.009	2.104	2.282
*M*8	1.783	1.867	2.024
*M*9	1.873	1.961	2.127
*M*10	1.703	1.783	1.933
O1	1.857	1.944	2.108
O2	1.801	1.886	2.045
O3	1.948	2.039	2.212
O4	1.941	2.032	2.204
O5	1.913	2.003	2.172
O6	1.948	2.040	2.212
O7	1.928	2.019	2.190
O8	1.849	1.936	2.099
O9	1.866	1.953	2.118
O10	1.885	1.973	2.140
O11	1.862	1.950	2.115
O12	1.932	2.023	2.194
O13	1.933	2.024	2.195
O14	1.990	2.083	2.259
O15	1.866	1.954	2.119
O16	2.098	2.164	2.289

very small atomic displacement parameters (model 2, Table 2). The *R* values at this stage were satisfactory and the calculation of bond-valence sums indicated a reasonable crystal chemistry, given the complexity of the structure. However, a number of factors indicated that this was not the model corresponding to the absolute minimum. The goodness-of-fit (GOF) was still relatively high (~4), merged data did not result in lower *R* values but higher GOFs than unmerged data and the final difference Fourier map showed quite considerable 'noise'. Furthermore, dividing reflections into various classes of satellites, see below, made it apparent that for some of the weaker classes of reflections the model was quite inadequate.

As the positions of metal and oxygen ions appeared to be correct the metal-ordering scheme was investigated more closely and without the assumption that as many sites as possible should be fully occupied by one or other metal-ion type. One metal site after another was subjected to mixing with the other metal-ion types and step-by-step a metal-ordering scheme emerged that was clearly distinguished from maximum order. In a final step the program *RAELS*95 (Rae, 1995) was used to refine the occupancies of all metal sites simultaneously, using appropriate constraints. With that refined metal-ordering pattern (model 3, Table 2) the final refinement allowed anisotropic displacement parameters for all sites, the GOF was low, *R* values were lower for merged data and the final difference Fourier map contained no large features. *R* values for the final result are $R = 0.031$ and $wR = 0.034$.

One of the major problems with the structure solution and refinement of this long-period superstructure is its essentially modulated character. A close look at the intensity distribution in reciprocal space shows that only a few types of reflections are observed strongly. These are the reflections that correspond either to the underlying fluorite-type parent structure or to the two types of satellite reflections thereof, *i.e.* characterized by the modulation wave vectors 404 and 913. It is difficult, however, to use a modulated structure approach owing to the fact that satellite reflections cannot be indexed unambiguously. The reflection classes are given in Table 3 with the percentage each contributes to the total intensity. It is evident that most of the scattered intensity is concentrated in the parent reflections and the first-order harmonics of types 404 and 913. It is important to note, however, that the division of reflections into classes is only a first-order approximation and neglects the fact that there are in principle an infinite number of combinations of the above modulations that lead to the same reflections. In fact, only parent reflections and first-order satellites (of types 404 and 913) are reasonably certain. Therefore, a description as a superstructure has been adopted despite its inherent over-parameterization of the refinement and subsequent introduction of 'noise' into the structural parameters (Withers *et al.*, 1998).

4. Results and discussion

4.1. *Results*

Final agreement indices of the refinement are given in Table 2, together with the various metal-ordering schemes. Coordinates and isotropic atomic displacement parameters are listed in Table 4, bond-valence sums in Table 5 and selected bond distances in Table 6.†

4.2. *Metal and oxygen-vacancy ordering*

Complete ordering of metal atoms is not possible in space group *Fddd* owing to the combination of 240 metal sites, stoichiometry and site multiplicities. The lowest multiplicity of any site in *Fddd* is 8, whereas a multiplicity of 4 is required for complete ordering of metals on individual sites. As discussed above, a metal-ordering scheme with full occupancies leads to the wrong stoichiometry (see Table 2), while a model with only two sites mixed appropriately yields the correct composition but not the best result. Finally, the best result has mixed occupancies on almost all metal sites. Projection of the structure along **b** (Figs. 2 and 3) reveals that there are only six different columns if one takes the average scattering of the two metal sites per unit cell that project on top of each other. Two of these columns have the

† Supplementary data for this paper are available from the IUCr electronic archives (Reference: BR0081). Services for accessing these data are described at the back of the journal.

Table 6. *Bond distances (Å)*

*M*1—O3	2.016 (7)	*M*2—O3	1.974 (7)	*M*3—O5	1.994 (6)
*M*1—O9	2.080 (6)	*M*2—O14	1.976 (7)	*M*3—O7	1.990 (6)
*M*1—O2	2.004 (6)	*M*2—O14	1.976 (7)	*M*3—O8	1.999 (5)
*M*1—O2	2.004 (6)	*M*2—O3	1.974 (7)	*M*3—O9	1.984 (6)
*M*1—O3	2.016 (7)	*M*2—O11	2.001 (7)	*M*3—O12	2.000 (3)
*M*1—O9	2.080 (6)	*M*2—O11	2.001 (7)	*M*3—O14	1.992 (7)
*M*4—O10	2.041 (5)	*M*5—O11	2.219 (7)	*M*6—O2	2.136 (6)
*M*4—O16	2.38 (1)	*M*5—O13	2.109 (7)	*M*6—O4	2.009 (8)
*M*4—O1	2.057 (3)	*M*5—O16	2.242 (6)	*M*6—O5	2.213 (6)
*M*4—O6	2.031 (7)	*M*5—O6	2.050 (7)	*M*6—O8	2.302 (7)
*M*4—O7	2.039 (6)	*M*5—O11	2.219 (7)	*M*6—O11	2.181 (7)
*M*4—O5	2.148 (6)	*M*5—O13	2.109 (7)	*M*6—O13	2.238 (7)
		*M*5—O16	2.242 (6)	*M*6—O8	2.179 (5)
		*M*5—O6	2.050 (7)		
*M*7—O3	2.683 (6)	*M*8—O2	2.486 (6)	*M*9—O9	2.401 (7)
*M*7—O4	2.173 (7)	*M*8—O6	2.387 (7)	*M*9—O12	2.596 (6)
*M*7—O5	2.773 (6)	*M*8—O7	2.619 (7)	*M*9—O15	2.238 (6)
*M*7—O9	2.770 (7)	*M*8—O8	2.543 (8)	*M*9—O14	2.862 (7)
*M*7—O10	2.481 (7)	*M*8—O4	2.374 (8)	*M*9—O9	2.401 (7)
*M*7—O15	2.170 (7)	*M*8—O11	2.711 (7)	*M*9—O12	2.596 (6)
*M*7—O7	2.477 (6)	*M*8—O3	2.558 (6)	*M*9—O15	2.238 (6)
*M*7—O14	2.472 (7)	*M*8—O4	2.304 (7)	*M*9—O14	2.862 (7)
*M*10—O1	2.456 (5)			O16—O16′	1.62 (2)
*M*10—O2	2.466 (6)				
*M*10—O6	2.483 (7)				
*M*10—O13	2.579 (7)				
*M*10—O1	2.456 (5)				
*M*10—O2	2.466 (6)				
*M*10—O6	2.483 (7)				
*M*10—O13	2.579 (7)				

same average number of electrons (34) whereas the others have 24, 45, 55 and 65 electrons. Fig. 3 shows that these columns are arranged in the following way. The isolated columns with low scattering power (24 e) are surrounded by a diamond of eight heavier-scattering columns, which are in turn almost enclosed by rows of lighter-scattering columns. The cells that are formed in this way are reminiscent of the *A*/*B* metal-atom and oxygen-vacancy ordering characteristic of the pyrochlore structure type with (111) planes of metal ions being alternately Ca rich and Ca poor (*cf.* Figs. 6 and 7 of Withers *et al.*, 1992). If such an ordering pattern was repeated indefinitely, sharp satellite reflections at $\mathbf{G}_F \pm \frac{1}{2}\langle 111\rangle_F^*$ would result. The reason for the satellite reflections moving to the $\mathbf{G}_F \pm [404]^*$ positions is the '*anti* phase boundaries' (dotted in Fig. 3) across which the phase of the metal-ion and oxygen-vacancy ordering changes by 180°. Such an *anti*-phase-boundary model has long been proposed as the reason for the rings of diffuse intensity around the $\mathbf{G}_F \pm \frac{1}{2}\langle 111\rangle_F^*$ positions in CSZs (van Dijk *et al.*, 1986; Miida *et al.*, 1994, 1997).

4.3. *Metal coordination spheres*

There are ten crystallographically independent metal sites (Fig. 4). Most of those are occupied by a mixture of two metals, therefore every site needs to be discussed individually. Ta and Zr in sites *M*1–*M*3 are coordinated by six O atoms in quite regular octahedra, while Ta and Zr in sites *M*4–*M*6 have both seven- and eightfold environments. Ca/Zr in sites *M*7–*M*10 have eightfold

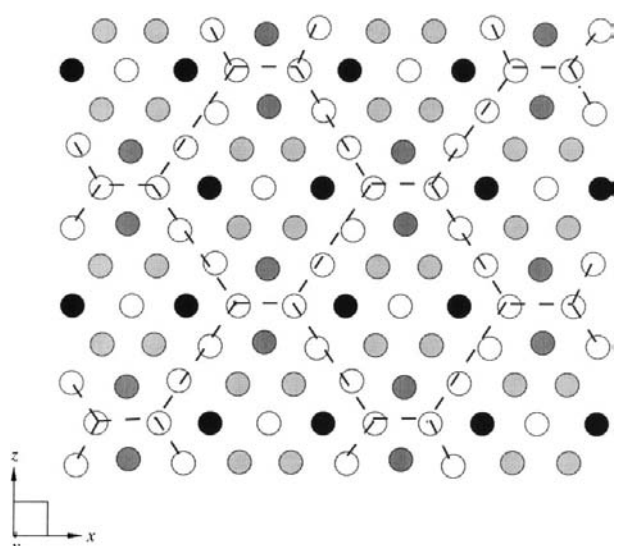

Fig. 3. Projection of the metal array down **b** with shading reflecting the average scattering power per column [white (isolated) 24, white (rows) 34, light grey 45, dark grey 55, black 65 e].

coordination representing slightly distorted cubes. Bond lengths are given in Table 6. It is evident that the polyhedra for each metal site are distinctly different, but mainly influenced by the major occupant.

Fig. 4 shows that some of the sites have quite anisotropic displacement parameters (*e.g.* *M*7, *M*9, O1) or very large displacement parameters (O16). These parameters can be explained by the disorder that necessarily accompanies the established metal-ion ordering pattern. In light of that disorder it is rather surprising that the structure refines as well as it does. Site *M*4, which has both O1 and O16 coordinated, is the only site where two

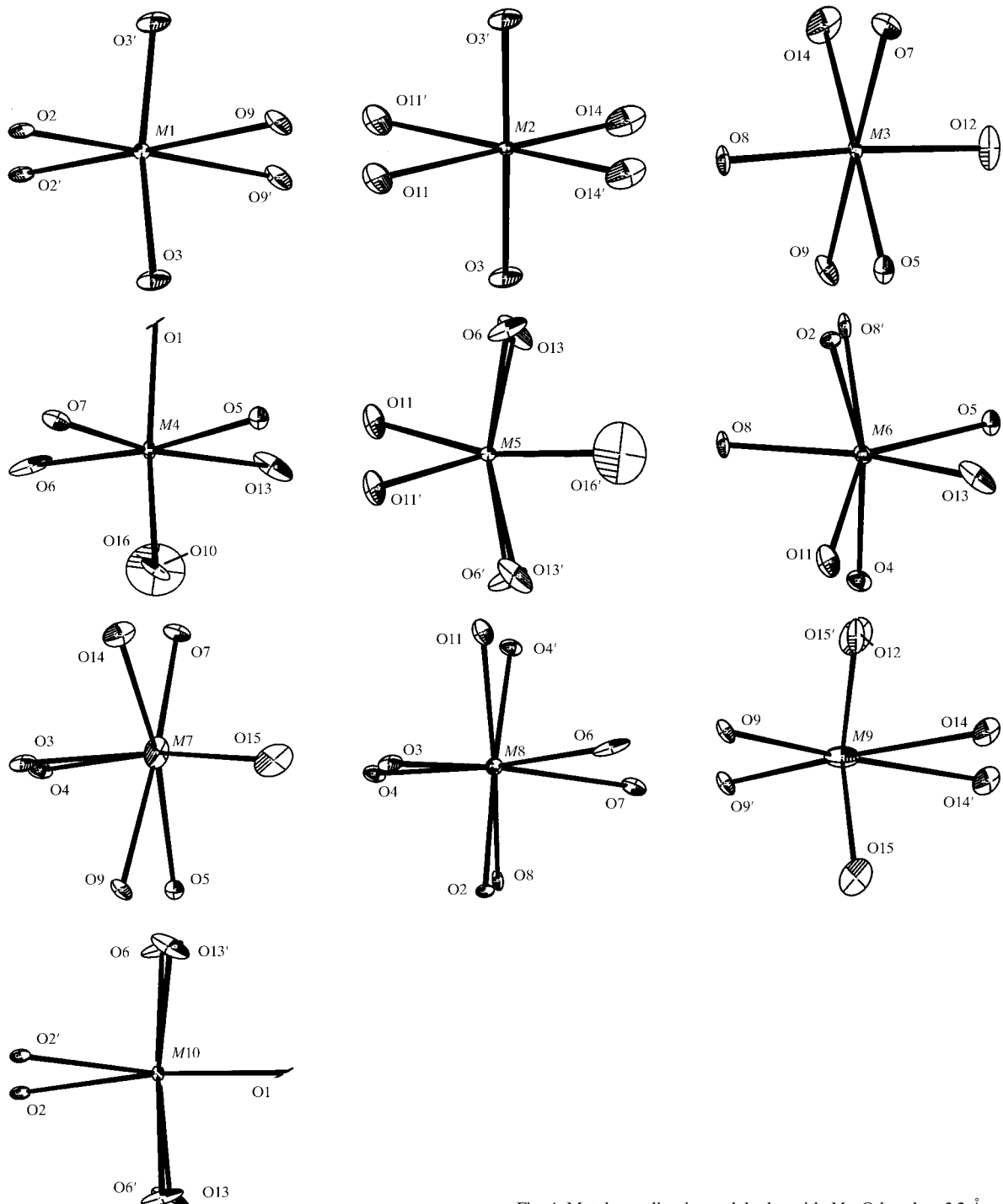

Fig. 4. Metal coordination polyhedra with $M-O$ bonds < 3.2 Å.

metals are mixed in almost equal proportions, thus explaining the behaviour of the displacement parameters for these O-atom sites. Furthermore, the site O16 has to be understood as the average site of a disordered O-atom position, as otherwise a bond from O16 to a symmetry equivalent results which is too short (see Table 6).

4.4. *Metal ordering and bond-valence sums*

Bond-valence sums (Brown & Altermatt, 1985; Brese & O'Keeffe, 1991) were calculated for metal and oxygen ions (Table 5) using the program *EUTAX* (Brese & O'Keeffe, 1991). These indicate that the structure is plausible. However, the numbers need to be interpreted with great care. The values given have been calculated assuming all cation sites are occupied by the same element. It is striking that all the O atoms have acceptable bond-valence sums independent of the nature of the coordinated metal atom. By contrast, the metal atoms appear to strongly favour different sites, *e.g.* sites *M*7–*M*10 can only be reasonably occupied by Ca, site *M*6 by Zr and sites *M*2 and *M*3 by Ta. For the remainder a mix of Ta and Zr is required to match the bond-valence sums. This and the refined metal-atom ordering require slight local rearrangements whenever one or the other metal atom occupies a particular site. For Ta and Zr the difference in expected valences is only 1, therefore only small adjustments are necessary. This difference is larger for Zr on sites that are mainly occupied by Ca; however, the high coordination number somewhat alleviates the impact. Rossell & Scott (1975) found that similar Ca/Hf disorder improved *R* values for the refinement of $Ca_2Hf_7O_{16}$.

To further establish the plausibility of the crystal chemistry a comparison with the bond-valence sums for $CaZr_4O_9$ (Marxreiter *et al.*, 1990) and $CaHf_4O_9$ (Allpress *et al.*, 1975) was sought. Diffraction patterns of $Ca_7Zr_7Ta_6O_{36}$ resemble some of the prominent features in diffraction patterns of these so-called φ^1 phases (Allpress *et al.*, 1975), presumably because of the existence of similar pyrochlore-like ordering in all of these structures. $CaZr_4O_9$ was refined from powder neutron data (Marxreiter *et al.*, 1990), while X-ray powder diffraction data were used for $CaHf_4O_9$ (Allpress *et al.*, 1975). Bond-valence sums revealed that the crystal chemistry for both fully ordered structures is less convincing than for $Ca_7Zr_7Ta_6O_{36}$, and in fact quite implausible for $CaZr_4O_9$ (Marxreiter *et al.*, 1990).

5. Conclusion

While compositional analysis and synthetic evidence point to this line phase having the simple stoichiometry $Ca_7Zr_7Ta_6O_{36}$, the structure refinement shows that in fact full ordering on metal-atom sites is not compatible with the established space-group symmetry nor with the diffraction data. Exactly why the phase should be a line phase is therefore not at all apparent. It is conceivable though that at the temperature of synthesis a high-temperature form exists, which allows for random disorder of the incorporated metal and oxygen atoms and which is partly preserved on quenching to room temperature. The refined structure of $Ca_7Zr_7Ta_6O_{36}$ may then be regarded as a frozen-in state of such a high-temperature form.

A major part of the experimental work was made possible by funding from the Australian Synchrotron Research Program of the Australian Federal Government and the generous allocation of beam time by the Photon Factory, National Laboratory for High Energy Physics, Tsukuba, Japan (Project No. 96G108). We acknowledge a Grant-in-Aid for International Scientific Research (Joint Research No. 08044132) from the Ministry of Education, Japan.

References

Allpress, J. G., Rossell, H. J. & Scott, H. G. (1975). *J. Solid State Chem.* **14**, 264–273.
Brese, N. E. & O'Keeffe, M. (1991). *Acta Cryst.* B**47**, 192–197.
Brown, I. D. & Altermatt, D. (1985). *Acta Cryst.* B**41**, 244–247.
Cromer, D. T. & Liberman, D. A. (1981). *Acta Cryst.* A**37**, 267–268.
Dijk, M. P. van, Mijlhoff, F. C. & Burggraaf, A. J. (1986). *J. Solid State Chem.* **62**, 377–385.
Hall, S. R., King, G. S. D. & Stewart, J. M. (1995). Editors. *Xtal*3.4 *User's Manual.* University of Western Australia, Perth: Lamb.
Kishimoto, S., Ishizawa, I. & Vaalsta, T. P. (1998). *Rev. Sci. Instrum.* **69**, 384–391.
Kissel, L. & Pratt, R. H. (1990). *Acta Cryst.* A**46**, 170–175.
Marxreiter, H., Boysen, H., Frey, F., Schulz, H. & Vogt, T. (1990). *Mater. Res. Bull.* **25**, 435–442.
Michel, D., Perez Y Jorba, M. & Colonques, R. (1974). *Mater. Res. Bull.* **9**, 1457–1468.
Miida, R., Sato, F., Tanaka, M., Naito, H. & Arashi, H. (1997). *J. Appl. Cryst.* **30**, 272–279.
Miida, R., Tanaka, M., Arashi, H. & Ishigame, M. (1994). *J. Appl. Cryst.* **27**, 67–73.
Rae, A. D. (1995). *RAELS*95. *Program for Constrained Least Squares Refinement.* Australian National University, Canberra, Australia.
Rossell, H. J. & Scott, H. G. (1975). *J. Solid State Chem.* **13**, 345–350.
Satow, Y. & Iitaka, Y. (1989). *Rev. Sci. Instrum.* **60**, 2390–2393.
Schmid, S., Lobo, C., Withers, R. L. & Thompson, J. G. (1996). *J. Solid State Chem.* **127**, 82–86.
Sheldrick, G. M. (1997). *SHELX*97. *Program for the Solution and Refinement of Crystal Structures*. University of Göttingen, Germany.
Withers, R. L., Schmid, S. & Thompson, J. G. (1998). *Prog. Solid State Chem.* **26**, 1–96.
Withers, R. L., Thompson, J. G., Barlow, P. J. & Barry, J. C. (1992). *Aust. J. Chem.* **45**, 1375–1395.